NERC-LV-539-21

PARTICULATE EFFLUENT STUDY
NRX-A6, EP-IIIA -- December 15, 1967

by
Environmental Surveillance
National Environmental Research Center

U. S. ENVIRONMENTAL PROTECTION AGENCY
Las Vegas, Nevada

Published March 1973

This study performed under a Memorandum of
Understanding No. AT(26-1)-539
for the
U. S. ATOMIC ENERGY COMMISSION

Available from the National Technical Information Service,
U. S. Department of Commerce,
Springfield, VA. 22151

Price: paper copy $3.00; microfiche $.95

NERC-LV-539-21

PARTICULATE EFFLUENT STUDY
NRX-A6, EP-IIIA -- December 15, 1967

by
Environmental Surveillance
National Environmental Research Center

U. S. ENVIRONMENTAL PROTECTION AGENCY
Las Vegas, Nevada

Published March 1973

This study performed under a Memorandum of
Understanding No. AT(26-1)-539
for the
U. S. ATOMIC ENERGY COMMISSION

ABSTRACT

The NRX-A6 Experimental Plan III was a full-power nuclear reactor operation conducted as part of Project Rover. The reactor ran from 1059 to 1159 PST, December 15, 1967 at the Nuclear Rocket Development Station, Jackass Flats, Nevada.

This report, covering information on large particles of high activity, includes particle deposition density at various distances; and gross physical characteristics, chemical composition, and gross and specific radioactivity of these particles.

Surveys along arcs out to a distance of 68 miles showed a peak deposition density at 15 miles of 1 particle/10 m^2. No particles were found beyond 40 miles from the reactor. At 40 miles the peak density was approximately 4 particles/100 m^2.

The particles were porous and fragile and had a metallic black appearance. Sizes ranged from two to 430 μ; some consisting of up to 3 discreet particles adhering to one another. Many of the particles were shattered during collection and separation from the soil with which they were collected.

The chemical composition of the particles was primarily UC_2 and various uranium oxides. In some cases alpha quartz was closely bound to the particles. The density of the material ranged from slightly less than one to 3.6.

Gross activity of the particles was 10^8 - 10^{12} fissions. Alpha activity was not determined because of the method of mounting the sample on glass slides with collodion. The primary radioisotopes found by gamma spectroscopy were those of Sr, Zr, Ru, I, Ba, Mo, and Ce.

TABLE OF CONTENTS

LIST OF TABLES

LIST OF FIGURES

I. INTRODUCTION

The NRX-A6 Experimental Plan III was conducted from 1059 to 1159 hours PST on December 15, 1967 as part of Project Rover operations by the Westinghouse Aerospace Nuclear Laboratory. The experiment was conducted at Test Cell C at the Nuclear Rocket Development Station. The reactor was operated at full power for 60 minutes (1100 Mw equivalent thermal).

Previous reactor tests, in particular Phoebus-1B EP-IV, resulted in effluent releases which included particulate matter. This report concerns work by the National Environmental Research Center-Las Vegas (NERC-LV)*, Environmental Protection Agency, as outlined in the Project Proposal for Reactor Effluent Studies - Particulate, dated August 1, 1967. Definitions of terms appear on Page 35.

*At the time this work was performed, the Center was named the Southwestern Radiological Health Laboratory and was part of the Public Health Service.

II. STUDY OBJECTIVES

The objectives presented in the Project Proposal which were pursued in this study were to determine:

The deposition concentration (particles per unit area) of particles both downwind and normal to the downwind axis.

The concentration hotline of deposited particles.

The physical, chemical, and radiometric parameters for isolated sources.

The particle size distribution for downwind distances.

An added objective was to compare collection methods used by the NERC-LV and Pan American field monitors.

III. FIELD ASSAY

A. Methods of Collection

Sampling routes were established in the downwind direction at approximately 11, 16, 25, 40, and 60 miles from Test Cell C following existing roads. The distances between sampling locations and areas of plots are listed in Table 1. Specific instructions were given to each sampling team, Appendix A.

Table 1. Arc data for sampling.

Arc (miles from Test Cell C)	Plot Area (M^2)	Number of Locations (along the arc)	Distance between locations (mi)
11	30	19	At PAA* stakes
16	30	38	0.5
25	30	17	0.5
40	50	29	1.0
60	80	51	1.0 & 2.0

*PAA - Pan American World Airways, Inc.

On the day of the reactor operation one location on Highway 95 was surveyed. On the day following the reactor operation two NERC-LV monitors and two PAA monitors collected particles along an 8-13 mile arc from Test Cell C. Eight other NERC-LV teams conducted particle searches along arcs from 16 to 68 miles from Test Cell C. The segments of the arcs to be surveyed were determined by preliminary ground monitoring and aircraft cloud tracking on the day of the event.

On Run + 1 (R + 1) day, after all arcs were sampled, an additional effort was made on the 16 mile arc to obtain particles for a special biological study.

B. Field Results

Survey results are presented in Tables 2 and 3. Table 2 presents results for on-site locations which were obtained while working on a side-by-side search with PAA. Initially 10 one-square-meter plots were surveyed at each location, but the number was increased to obtain additional particles. Table 3 presents results for off-site locations. Both tables give azimuth and distance of the location from Test Cell C, total particles found at a location, and the particle concentration. In the off-site search, a few particles were located outside the required plot area. These are so noted in the last column. These finds were recorded for information only as the particles were not included in the deposition concentration, nor were they collected.

The sampling locations and particle concentrations from Table 2 and 3 are presented in Figure 1. A particle hotline approximately 219° as determined from these is also indicated in Figure 1.

A three dimensional representation of the particle deposition concentration is shown in Figure 2. The concentration has been normalized to particles per square meter. The number of particles located on the survey was sufficient to define the hotline, but insufficient to define cross wind distributions past the 15-mile arc. The change in average deposition concentration with distance is shown in Figure 3. Curve A is the ratio of the total number of particles found along an arc to the total positive plot area versus distance from Test Cell C, while Curve B is the ratio of the total number of particles found along an arc to the total plot area between edges of the deposition pattern. Both curves indicate a maximum concentration peak at 15 miles.

Table 2. Particle survey location--on-site locations(PAA stake numbers).

Date Collected	Location Stake No.	Azimuth from Test Cell C	Distance (miles)	No. Part. per area surveyed	Particle Conc. (particles/m^2)	Particles* found outside template
12/16/67	93	238°	11	0/30 m^2	0.0	-
"	94	235°	11	0/30 m^2	0.0	-
"	95	233°	11	0/30 m^2	0.0	-
"	96	230°	12	0/30 m^2	0.0	-
"	97	226°	12	1/30 m^2	0.033	-
"	98	222°	13	1/30 m^2	0.033	-
"	99	219°	13	0/30 m^2	0.0	-
"	110	232°	8	0/30 m^2	0.0	-
"	111	226°	9	2/30 m^2	0.067	-
"	112	222°	11	5/30 m^2	0.167	-
"	113	219°	12	4/30 m^2	0.133	-
"	114	217°	13	1/30 m^2	0.033	-
"	115	215°	13	0/10 m^2	0.0	-
"	116	213°	13	1/10 m^2	0.1	-
"	117	212°	12	0/10 m^2	0.0	-
"	118	210°	12	1/10 m^2	0.1	-
"	119	209°	12	0/10 m^2	0.0	-
"	120	208°	12	0/30 m^2	0.0	-
"	121	207°	12	0/30 m^2	0.0	-

*---not reported

Table 3. Particle survey locations - off-site locations.

Date Collected	Location	Azimuth from Test Cell C	Distance (miles)	No. Part. per area surveyed	Particle Conc. (particles / m^2)	Particles* found outside template
12/16/67	Lathrop Wells	208°	15	0/30 m^2	0.0	No
"	0.5 mi N Lathrop Wells on Hwy 95	212°	15	0/30 m^2	0.0	No
"	1 mi N Lathrop Wells on Hwy 95	214°	15	0/30 m^2	0.0	No
"	1.5 mi N Lathrop Wells on Hwy 95	215°	15	0/30 m^2	0.0	Yes
"	2 mi N on Hwy 95	216°	15	1/30 m^2	0.033	-
"	2.5 mi N Lathrop Wells on Hwy 95	218°	15.5	4/30 m^2	0.133	-
"	3 mi N Lathrop Wells on Hwy 95	219°	15.5	6/30 m^2	0.2	-
"	3.5 mi N Lathrop Wells on Hwy 95	221°	16	3/30 m^2	0.1	Yes
"	4 mi N Lathrop Wells on Hwy 95	223°	16	1/30 m^2	0.033	Yes
"	4.5 mi N Lathrop Wells on Hwy 95	224°	16.5	0/30 m^2	0.0	Yes
"	5 mi N Lathrop Wells on Hwy 95	226°	16.5	0/30 m^2	0.0	Yes
"	5.5 mi N Lathrop Wells on Hwy 95	227°	17	0/30 m^2	0.0	No
"	6 mi N Lathrop Wells on Hwy 95	229°	17	0/30 m^2	0.0	No
"	6.5 mi N Lathrop Wells on Hwy 95	230°	17.5	0/30 m^2	0.0	No
"	7 mi N Lathrop Wells on Hwy 95	231°	17.5	0/30 m^2	0.0	No
"	7.5 mi N Lathrop Wells on Hwy 95	233°	18	0/30 m^2	0.0	No

*Not reported

Table 3. Particle survey locations - off-site locations. (continued)

Date Collected	Location	Azimuth from Test Cell C	Distance (miles)	No. Part. per area surveyed	Particle Conc. (particles / m^2)	Particles found outside template
12/16/67	8 mi N Lathrop Wells on Hwy 95	234°	18	0/30 m^2	0.0	No
"	8.5 mi N Lathrop Wells on Hwy 95	235°	18.5	0/30 m^2	0.0	No
"	9 mi N Lathrop Wells on Hwy 95	237°	18.5	0/30 m^2	0.0	No
"	9.5 mi N Lathrop Wells on Hwy 95	238°	19	0/30 m^2	0.0	No
"	10.5 mi N Lathrop Wells on Hwy 95	240°	19.5	0/30 m^2	0.0	No
"	11 mi N Lathrop Wells on Hwy 95	242°	19.5	0/30 m^2	0.0	No
"	11.5 mi N Lathrop Wells on Hwy 95	244°	20	0/30 m^2	0.0	No
"	12 mi N Lathrop Wells on Hwy 95	245°	20	0/30 m^2	0.0	No
"	12.5 mi N Lathrop Wells on Hwy 95	246°	20	0/30 m^2	0.0	No
"	13 mi N Lathrop Wells on Hwy 95	248°	20.5	0/30 m^2	0.0	No
"	13.5 mi N Lathrop Wells on Hwy 95	249°	21	0/30 m^2	0.0	No
"	14 mi N Lathrop Wells on Hwy 95	250°	21	0/30 m^2	0.0	No
"	14.5 mi N Lathrop Wells on Hwy 95	251°	21.5	0/30 m^2	0.0	No
"	15 mi N Lathrop Wells on Hwy 95	253°	21.5	0/30 m^2	0.0	No
"	Junction Hwy 95 & Crater Flat Road	253°	21.5	0/30 m^2	0.0	-

Table 3. Particle survey locations - off-site locations. (continued)

Date Collected	Location	Azimuth from Test Cell C	Distance (miles)	No. Part. per area surveyed	Particle Conc. (particles / m^2)	Particles found outside template
12/16/67	0.5 mi N Crater Flat Road	254°	21	0/30 m^2	0.0	-
"	1 mi N Crater Flat Road	255°	21	0/30 m^2	0.0	-
"	1.5 mi N Crater Flat Road	255.5°	20	0/30 m^2	0.0	-
"	2 mi N Crater Flat Road	256°	20	0/30 m^2	0.0	-
"	2.5 mi N Crater Flat Road	257°	19.5	0/30 m^2	0.0	-
"	3 mi N Crater Flat Road	258°	19.5	0/30 m^2	0.0	-
"	3.5 mi N Crater Flat Road	260°	19	0/30 m^2	0.0	-
"	4 mi N Crater Flat Road	262°	19	0/30 m^2	0.0	-
"	2 mi W Hwy 29 on Amargosa Road	204°	23.5	1/30 m^2	0.033	-
"	4 mi W Hwy 29 on Amargosa Road	209°	24	1/30 m^2	0.033	-
"	7 mi W Hwy 29 on Amargosa Road	215°	25.5	1/30 m^2	0.033	-
"	7.5 mi W Hwy 29 on Amargosa Road	216°	25.8	3/30 m^2	0.1	-
"	8 mi W Hwy 29 on Amargosa Road	217°	25.5	2/30 m^2	0.067	-
"	8 mi W, 1 mi NW on Amargosa Road	219°	25	3/30 m^2	0.1	-
"	9 mi W, 2 mi NW on Amargosa Road	220°	25	0/30 m^2	0.0	-

Table 3. Particle survey locations - off-site locations. (continued)

Date Collected	Location	Azimuth from Test Cell C	Distance (miles)	No. Part. per area surveyed	Particle Conc. (particles / m^2)	Particles found outside template
12/16/67	8 mi W, 3 mi NW on Amargosa Road	222°	24.5	0/30 m^2	0.0	-
"	8 mi W, 4 mi NW on Amargosa Road	224°	24	1/30 m^2	0.033	-
"	8 mi W, 5 mi NW on Amargosa Road	226°	23.5	0/30 m^2	0.0	-
"	8 mi W, 6 mi NW on Amargosa Road	228°	23	0/30 m^2	0.0	-
"	8 mi W, 7 mi NW on Amargosa Road	231°	23	1/30 m^2	0.033	-
"	8 mi W, 8 mi NW on Amargosa Road	233°	23	0/30 m^2	0.0	-
"	8 mi W, 9 mi NW on Amargosa Road	235°	22.5	0/30 m^2	0.0	-
"	8 mi W, 10 mi NW on Amargosa Road	237°	22.5	0/30 m^2	0.0	-
"	From DVJ to 15 mi NW on 190	191-215°	37	0/50 m^2	0.0	-
"	16 mi NW DVJ on 190	216°	38	2/50 m^2	0.04	-
"	17 mi NW DVJ on 190	217°	39	1/50 m^2	0.02	Yes
"	18 mi NW DVJ on 190	217°	40	0/50 m^2	0.0	-
"	19 mi NW DVJ on 190	219°	40	0/50 m^2	0.0	Yes
"	20 mi NW DVJ on 190	221°	40	1/50 m^2	0.02	-
"	21 mi NW DVJ on 190	222°	40	5/50 m^2	0.10	-

Table 3. Particle survey locations - off-site locations. (continued)

Date Collected	Location	Azimuth from Test Cell C	Distance (miles)	No. Part. per area surveyed	Particle Conc. (particles / m^2)	Particles found outside template
12/16/67	20-30 mi NW DVJ on 190	224-234°	40	0/50 m^2	0.0	-
"	Between Trail Canyon in Death Valley and Shoshone at 1 and 2 mi intervals	181-228°	52-68	0/80 m^2	0.0	-

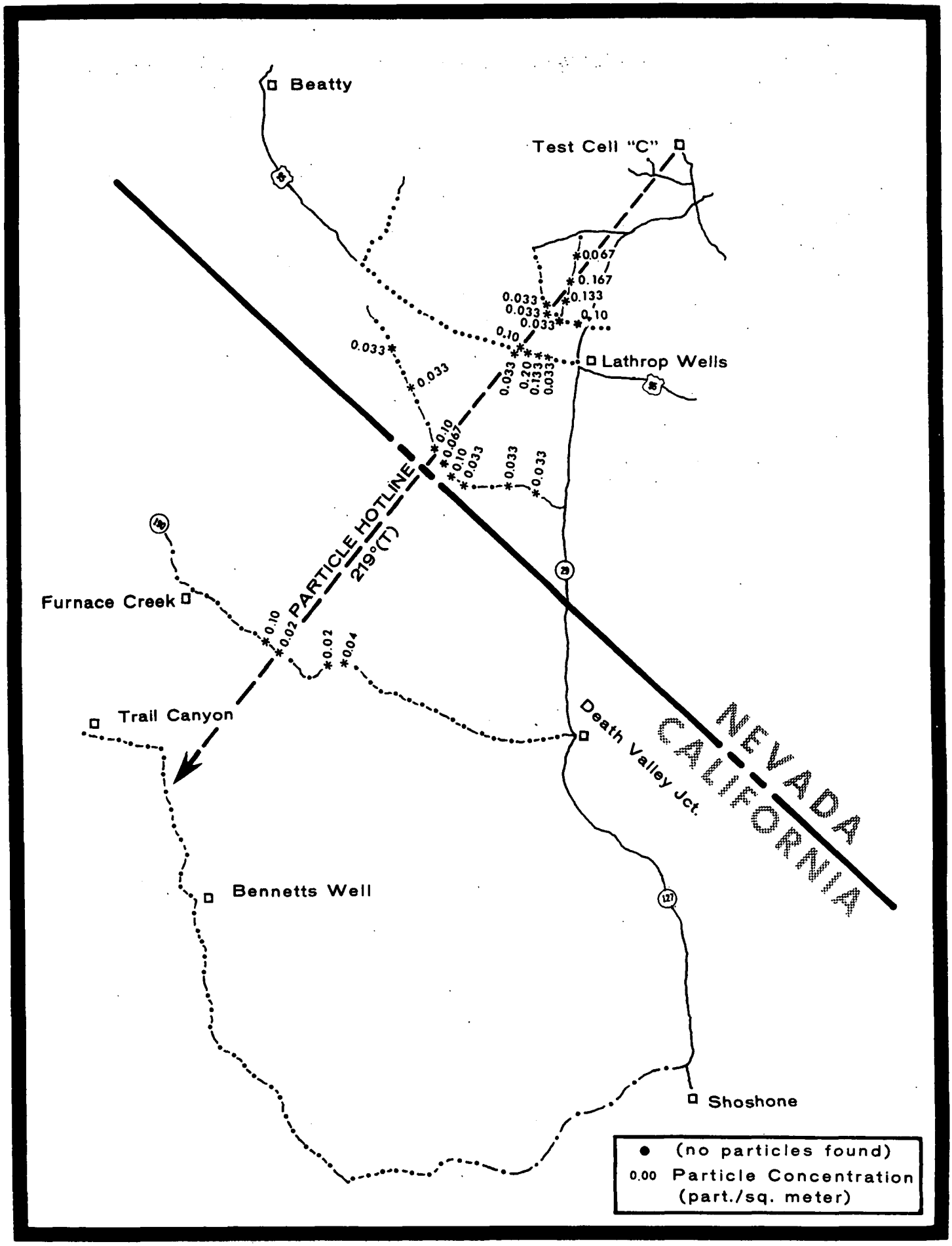

Figure 1. Survey results.

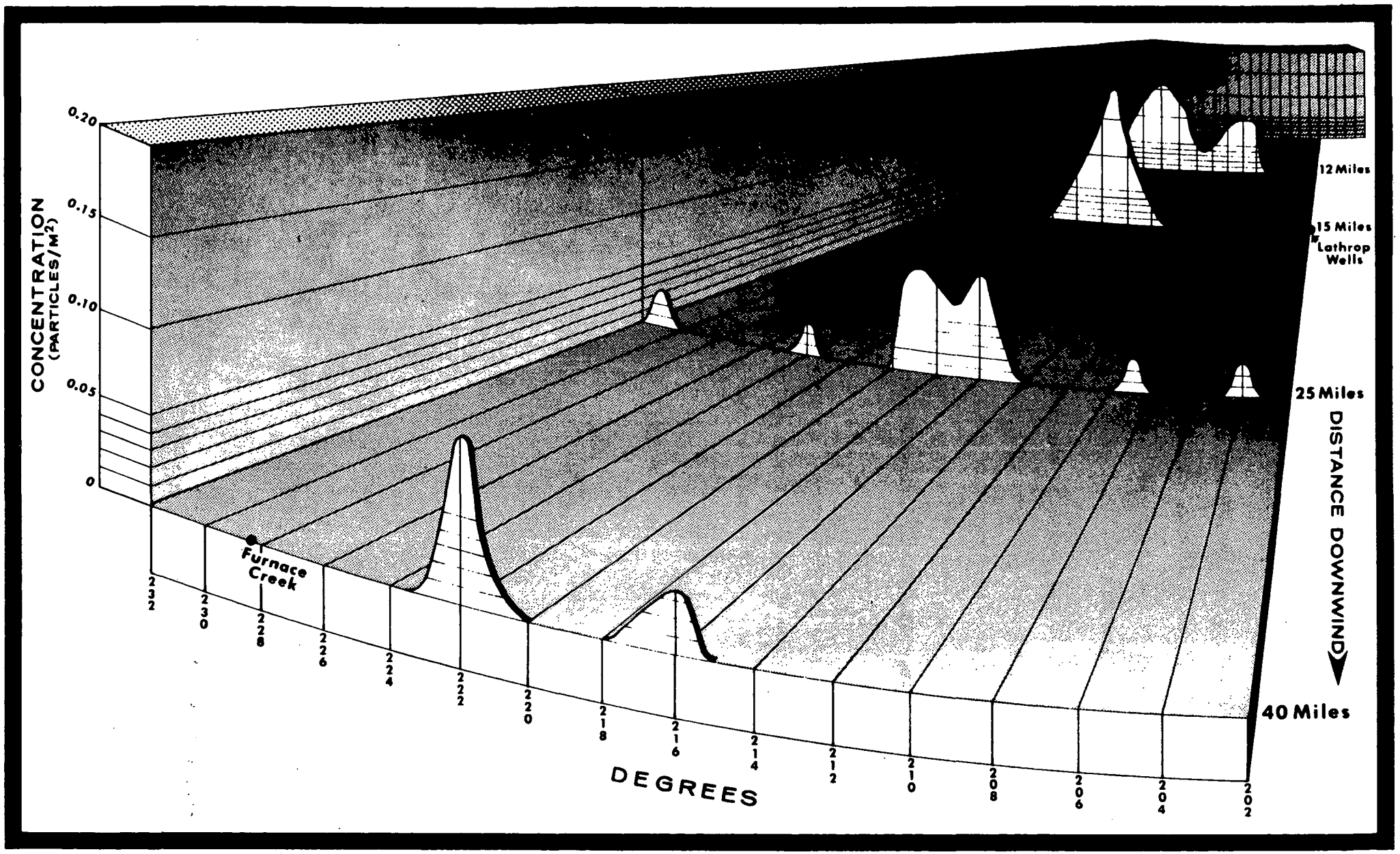

Figure 2. Survey results in three-dimensional representation.

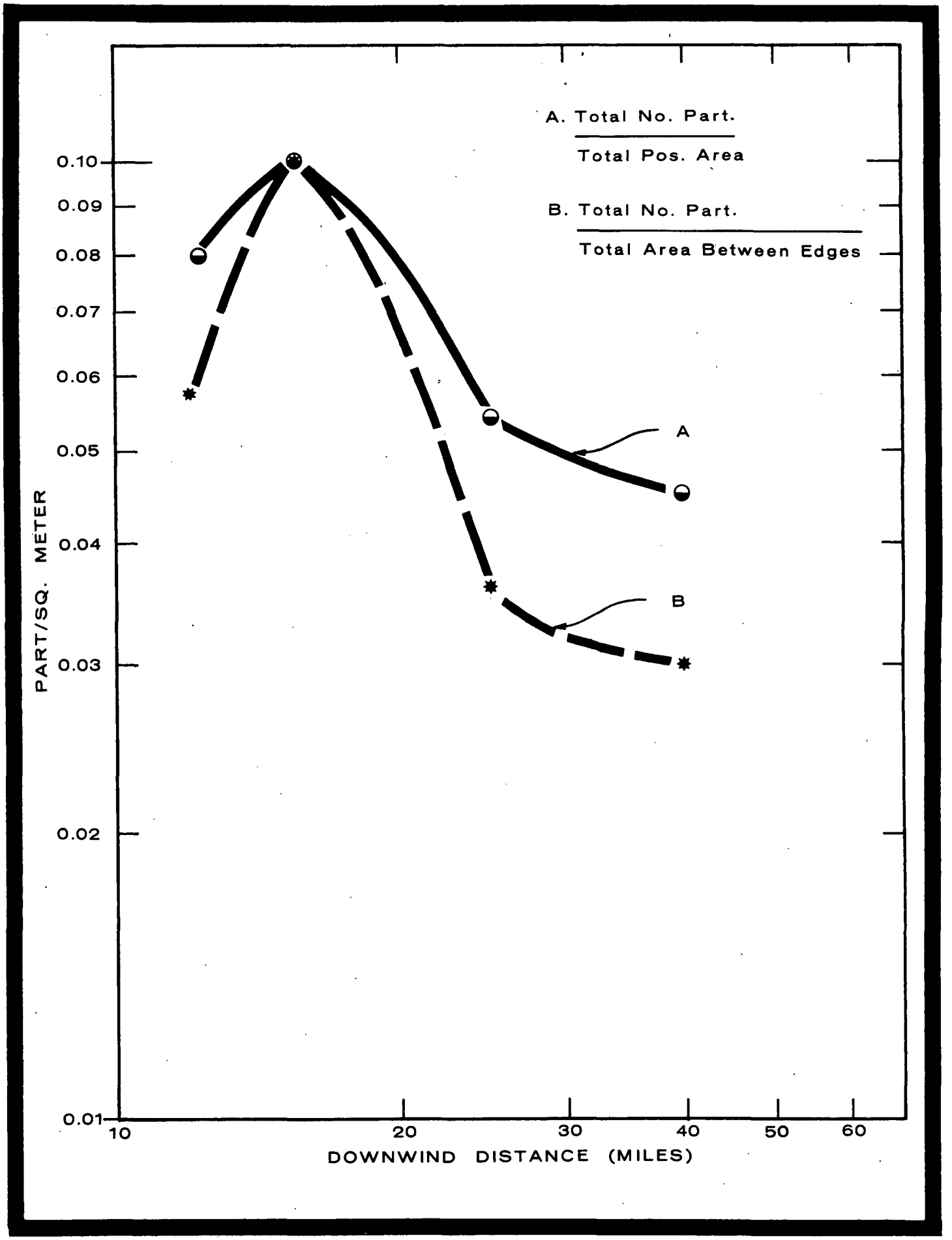

Figure 3. Deposition concentration versus distance.

C. Discussion of Field Results

The field results, as presented, are about what was expected, (Ref. 1). Correlation of the field data with weather data(Ref. 4) indicates that large particulate material was ejected from the reactor during the latter part of the run.

The length of the run and wind shear during the run may explain the bi-modal patterns (Figure 2) at all but the 15-mile arc. The patterns may also be a result of the intermittent rain and snow showers during the run. The peak concentration at the 15-mile arc (Figure 3) follows the same general pattern as observed on the Phoebus 1B EP-IV test.

Several samples were collected for a special biological study. Since the concentration of particles was so low, no attempt was made to determine the area from which the particles were collected.

IV. LABORATORY ANALYSIS

All samples were returned to the NERC-LV for analysis. After the radioactive material was separated from the matrix, its physical characteristics were determined. On selected samples radiometric and microprobe analysis was performed.

A. Separation

Initial separation was done by subdividing the sample into small portions and checking each portion with a lab monitor. The portions containing activity were mounted on 1-by 3-inch glass slides as "specimens."

All samples yielded more than one portion containing activity. As many as 26 specimens were obtained from a single sample. These specimens were identified as sub parts of the sample, i.e., 202A, 202B, etc. A radioautograph technique described in Appendix B indicated several radioactive spots on many specimens. Figure 4 is a photomicrograph of one that appears to be a bead or shell. Figures 5 and 6 show specimens of shattered beads or shells.

B. Physical Characteristics

The appearance of the radioactive material (when viewed under the microscope) varied considerably. Some pieces appeared black or metallic, some appeared porous, while others looked like black flakes adhering to colorless sand particles. A few pieces were spherical and in some cases were clustered into 2 or 3 beads. These beads were in the 50-100μ range.

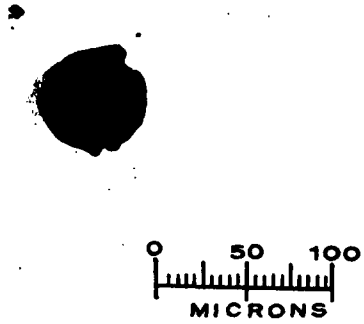

REACTOR BEAD
FIGURE 4

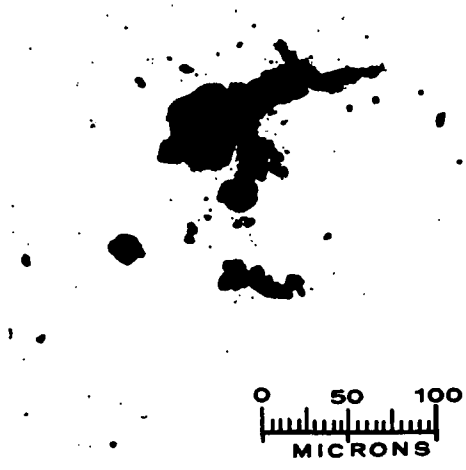

SHATTERED BEAD
FIGURE 5

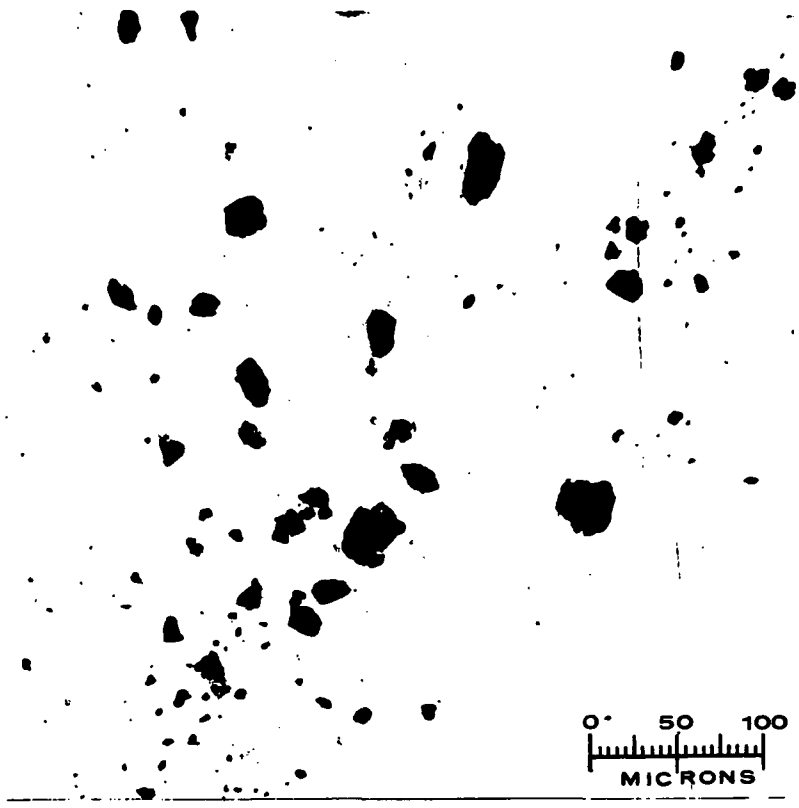

SHATTERED BEAD
FIGURE 6

All the pieces identified under the microscope were sized with the exception of those that were attached to what appeared to be sand particles. These are noted as "f/s" (flakes on sand). The dimensions of the pieces measured are reported as the maximum dimension and dimension perpendicular to it, reported in Table 1, Appendix C.

The particles collected for the biological study were isolated and sized. These data are reported in Table 2 of Appendix C.

Density analysis was performed on ten particles which were selected on the basis of shape and activity. The weights of the particles were determined by using a balance boat, described in Appendix D. Mass measurements were obtained on six of the particles as the other four appeared to be too fragile and breakage may have occurred.

The particles were then dropped into a column containing ethyl alcohol to measure their settling velocity as described in Appendix D. Each particle was timed by two separate watches and the average time reported. Specimen 207 was not observed to fall from the slide. Specimens 235 and 204H shattered as they fell through the solution.

Each particle was sized again before weighing. The size given is the maximum dimension and the dimension perpendicular to the maximum dimension. These size data may be different from those reported in Table 1, Appendix C, because of the reorientation of the particle from the original slide and/or the amount of collodion used in mounting. Data from the selected particles are reported in Table 4. The density ranged from 0.95 to 3.6 gm/cc with an average of 2.7 gm/cc.

Table 4. Results of density analysis.

Sample No.	Size (μ)	Weight (μg)	Distance of Fall(cm)	Time of Fall (sec)	Fall Velocity (cm/sec)	Density (gm/cc)
202B	234x225	8.00	21.11	13	1.6	2.1
204E	131x168	-	21.11	75.5	0.28	1.4
204J	112x122	-	21.11	25	0.84	3.6
205H	140x117	2.25	21.11	28	0.75	2.9
207	126x108	0.50	21.11	-	-	-
213D	187x173	8.75	21.11	12	1.76	3.2
220A	323x225	8.25	21.11	23.5	0.90	1.3
238B	347x328	25.5	21.11	51.5	0.41	0.95

- = Not observed
Viscosity of Liquid = 2.49 cp

Standard particles were used to calibrate the solution before the analysis was performed. The particles used were whole reactor beads, spherical in shape. The data obtained from these calibration particles are reported in Table 1, Appendix D.

C. Radiometric Analysis

All specimens were beta counted and gamma scanned. Beta counting was done on each specimen while the gamma scanning was done on individual specimens and groups of specimens from the same sample. There were no dissimilar data observed in this method. The groups of specimens method was used to decrease the time necessary for counting. Due to the method of mounting the particles, covered with 30% collodion solution, alpha counting was not attempted.

Beta activity, as of December 27 (R + 12), is reported in dpm, fissions, and picocuries for individual specimens in Table 1 of Appendix C. The activity for the sample, i.e., sum of individual specimen activities from the same sample, is listed in Table 5 along with the location of the samples (Azimuth and Distance from Test Cell C). Fifteen specimens were beta counted over an extended period of time to follow the decay and to determine the average maximum beta energy. Decay curves of the samples plotted on log-log paper had essentially the same shape and slope, indicating sample homogeniety. Comparison of the decay curves with published data (Ref. 5) indicates fair agreement with fission product decay, Figure 7.

Beta absorption tests, using aluminum absorbers, were run on the fifteen specimens at various times to determine average maximum beta energy (average of the maximum beta energies in the specimen). The average maximum beta energy for each specimen was determined from the half-thickness value of aluminum absorbers and was used to select the beta counting efficiency. All absorption curves exhibited essentially the same shape as that shown in Figure 8. The average maximum beta energy for the specimens was determined to be about 1.1 MeV and no trends were observed as a function of age. The average maximum beta energy is in fair agreement with the 1.2 MeV reported in the literature (Ref. 6). Calibration and other pertinent data concerning the beta counting data are given in Appendix C.

Specimens were gamma scanned on a multichannel analyzer with a 4-by 4-inch NaI(Tl) detector. Analyses of data were

Table 5. Activity and location of samples.

Arc	Sample No.	dpm	pCi E03*	Fissions E09**	Location Azimuth (°True)	Location Distance (Mile)
11 Mile	200	94,000	42	9	210	12
	201	110,000	50	10	217	13
	202	49,000	22	5	213	13
	203	220,000	99	20	222	13
	204	33,000,000	15,000	3,200	222	11
	205	29,000,000	13,000	2,800	222	11
	206	5,100,000	2,200	500	222	11
	207	6,000,000	2,700	550	222	11
	208	1,600	0.7	0.2	219	12
	209	5,000,000	2,200	460	219	12
	210	160,000	74	15	219	12
	211	31,000,000	14,000	2,900	219	12
	212	37,000,000	17,000	3,500	226	9
	213	15,000,000	7,000	1,400	226	9
	214	150,000	65	14	226	12
15 Mile	215	230,000	100	22	216	15
	216	1,100	0.5	0.1	219	15.5
	217	6,000	3	0.6	219	15.5
	218	63,000	28	7	219	15.5
	219	18,000,000	8,100	1,800	218	15.5
	220	210,000	96	20	218	15.5
	221	120,000	52	11	218	15.5
	222	130,000	59	12	218	15.5
	223	170,000	75	15	223	16
	224	2,000,000	900	190	221	16
	225	440,000	200	41	221	16

Table 5. Activity and location of samples. (continued)

Arc	Sample No.	dpm	pCi E03*	Fissions E09**	Location Azimuth (°True)	Location Distance (Mile)
25 Mile	226	5,600	3	0.5	231	23
	227	1,200	0.6	0.1	219	25
	228	670,000	220	62	219	25
	229	3,000	1	0.3	219	25
	230	22,000	10	2	204	23.5
	231	2,100,000	950	190	217	25.5
	232	35,000	16	3	216	25.75
	233	5,600,000	2,500	520	216	25.75
	234	4,000,000	1,800	470	217	25.5
	235	140,000	63	13	209	24
	236	91,000	41	9	215	25.5
	237	60,000	27	16	216	25.75
	238	4,600	2	0.4	224	24
40 Mile	239	29,000	13	3	216	38
	240	1,700,000	760	160	217	39
	241	130,000	59	12	221	40
	242	22,000	10	2	222	40
	243	3,400	2	0.3	222	40
	244	3,200	2	0.3	222	40
	245	4,600	2	0.4	222	40
	246	50,000	23	5	222	40

*E03 = 10^3

**E09 = 10^9

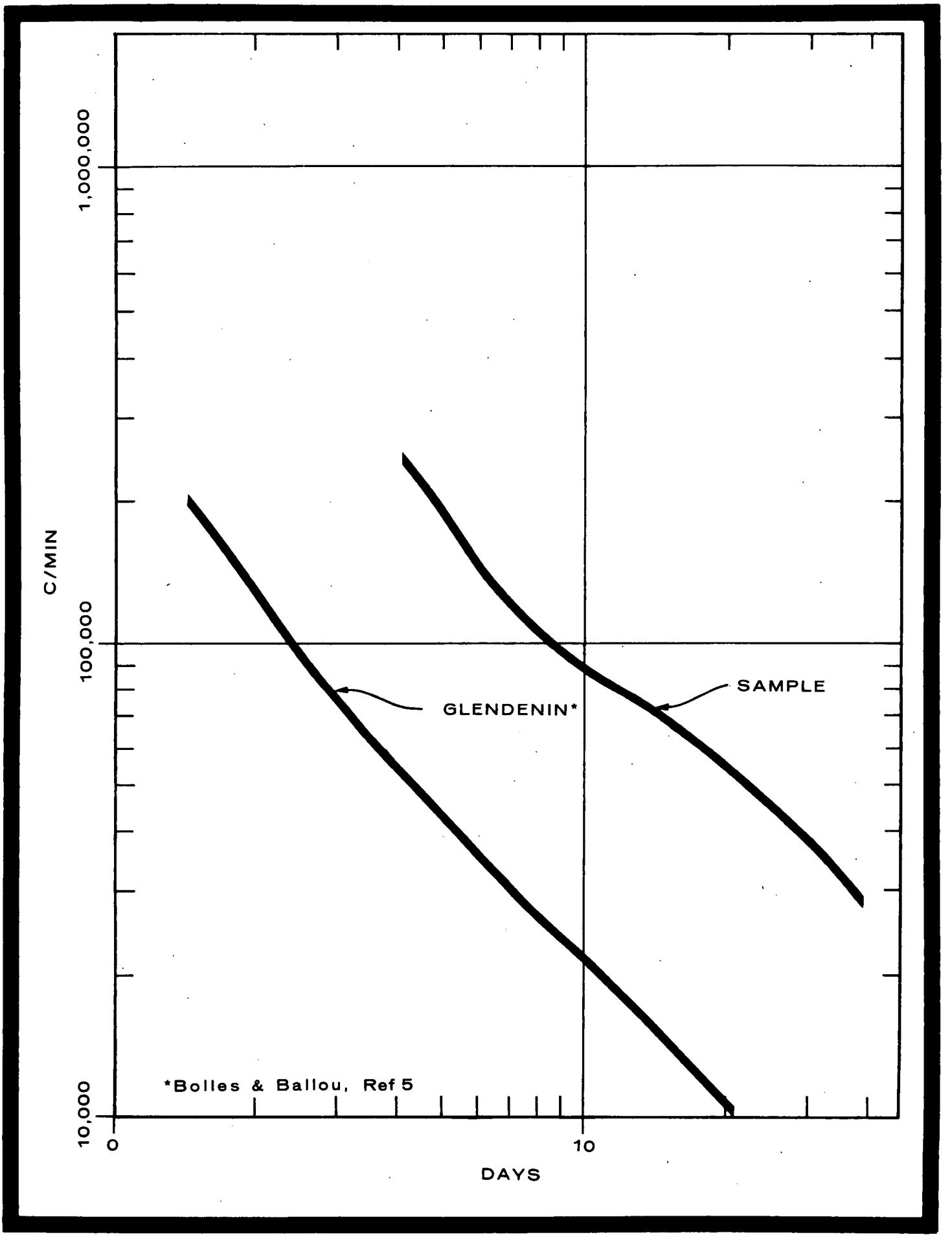

Figure 7. Comparison of beta decays.

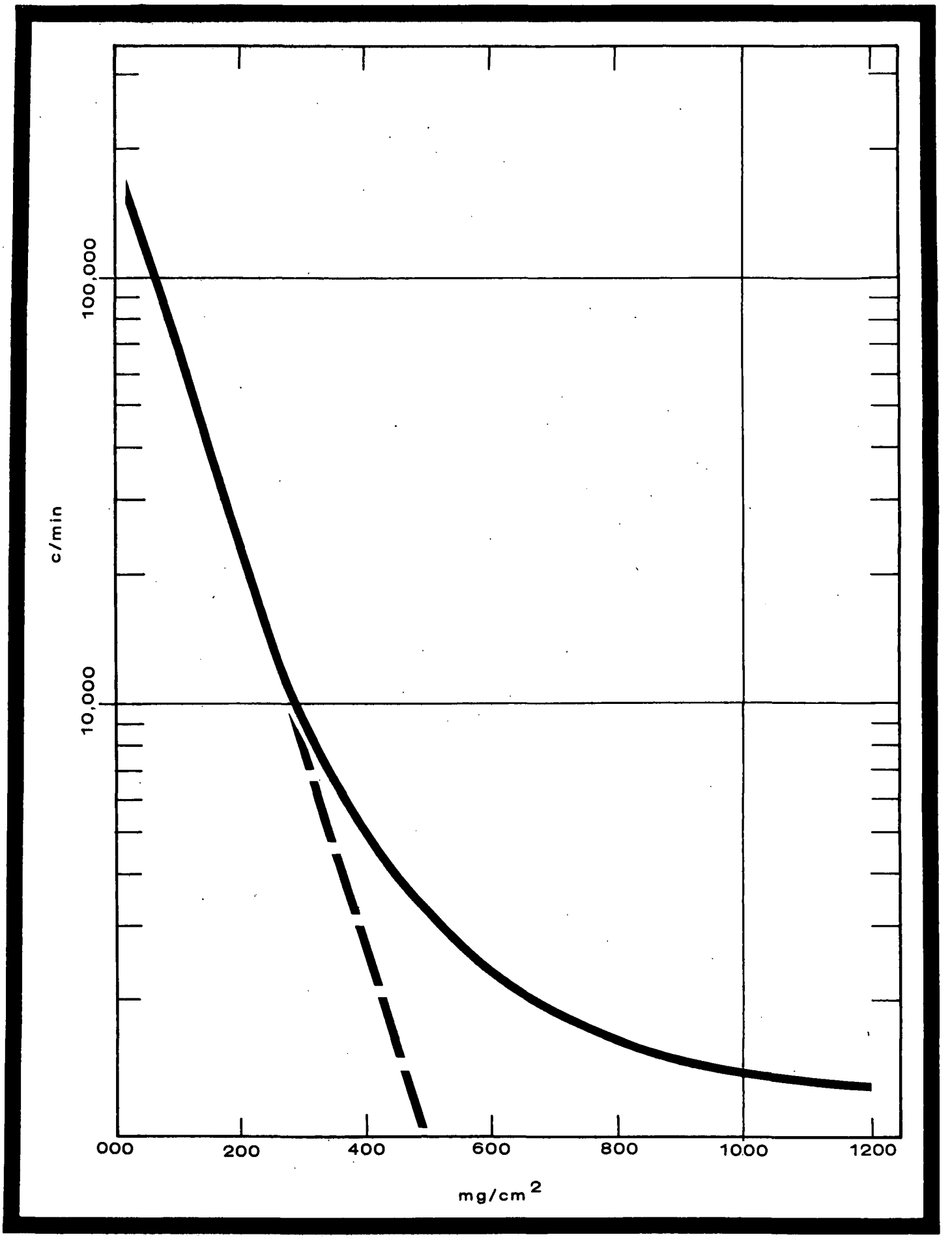

Figure 8. Typical beta absorbtion curve.

performed by two methods. Four randomly selected specimens were analyzed by hand methods using a series of gamma scans to obtain qualitative and quantitative information. The qualitative information was used to make up a library for the least squares method for quantitative analysis on the remainder of the specimens.

Comparisons of data results from both methods are presented in Table 6. Results generally agree by much less than a factor of two. The isotopes with the lower activities and poorer counting statistics show the worst agreement.

The isotopic data for each specimen are reported in Table 3 of Appendix C. These data have been extrapolated to 1200 hours on run day.

In some cases the specimens were too active to give good results with the least squares method of calculation. These specimens are marked with an asterisk. The high count rate associated with these specimens probably caused a gain shift in the spectrum which exceeded the limits of the program. Activities were calculated, but residual spectra and error terms were too high to meet the criteria for acceptance of the calculations. Hand calculations on these scans were performed to complete the data. Error values cannot be given for the method, but can be given for individual isotopes. In general, the error associated with each value was $\pm 25\%$.

D. Microprobe Analysis

Electron microprobe data and x-ray diffraction data were collected on a series of selected specimens containing particulate material which exhibited various levels of radioactivity.

Table 6. Comparison of data analysis methods*.

Specimen No.	218-A		226-B		227-A		243	
Method of Calculation	Hand	Computer	Hand	Computer	Hand	Computer	Hand	Computer
Isotope								
^{91}Sr	1.7 E04	4.4 E04	4.9 E04	5.1 E04	9.3 E03	1.2 E04	9.5 E04	6.7 E04
^{95}Zr	-	-	-	-	-	-	4.4 E03	2.6 E03
^{97}Zr	-	-	8.4 E03	4.0 E03	-	-	2.0 E05	1.7 E05
^{99}Mo	1.8 E04	1.2 E04	3.4 E03	2.5 E03	5.9 E03	8.6 E03	2.7 E04	1.5 E04
^{103}Ru	-	-	-	-	-	-	2.3 E03	1.8 E03
^{131}I	1.1 E03	1.3 E03	4.7 E02	6.1 E02	5.2 E02	3.9 E02	-	-
$^{132}Te-I$	1.1 E03	1.4 E03	2.6 E03	2.8 E03	ND	1.6 E02	-	-
^{133}I	3.1 E04	5.7 E03	ND	4.0 E03	6.4 E03	3.6 E03	-	-
^{135}I	-	-	7.5 E03	1.5 E04	-	-	2.9 E04	ND
$^{140}Ba-La$	1.2 E03	5.6 E02	1.2 E03	4.0 E02	-	-	ND	1.5 E02
^{141}Ce	2.8 E02	1.2 E02	2.9 E02	1.2 E02	-	-	8.4 E02	3.8 E02
^{143}Ce	-	-	-	-	-	-	3.6 E04	4.9 E04

*Activity (pCi @ 1200 hours 12-15-67)
- Not present
ND - Not detected
E04 = 10^4

The purpose of the microprobe examination was to determine the elemental composition of the sample. The purpose of the X-ray diffraction analysis was to determine the type of material which was exhibiting the radioactivity and to determine the chemical composition of the fragments.

Electron microprobe and X-ray diffraction analyses were done on specimens 224B and 205A. Electron microprobe analysis only was done on 233, 236, and 228B, because these specimens were lost in transferring from one system to the other. The data are reported in Table 7. Several fragments were located on each slide by radioautography. Each piece was individually analyzed.

E. Discussion of Laboratory Results

The relatively large particle sizes reported in Table 1, Appendix C, appear to be reactor material adhering to sand particles. This was verified by the electron microprobe; alpha quartz was the basic matrix, and in the density tests, lower densities were observed than would be expected for compounds of uranium, carbon, and oxygen.

The density data, although lower than expected, (uranium compounds should have density greater than 7.3 gm/cc) appear to be valid. The low values may be due to a combination of reasons. It is known that for sizes greater than 50μ, a departure from Stokes velocity occurs. Although this difference is not sufficient to account for the lower densities reported, it may be one source of error. The shape of the particles, porous appearance, and adherence to sand particles may also account for the lower values. A method of separating the reactor material from desert sand was

Table 7. Microprobe and X-ray diffraction data.

Specimen No.	Particle No.	Elements	Compounds	Particle Size
224 B	1	Si, Ca, K, O & S	alpha-Quartz	10 x 18 microns
	2	Si, Na, K, Ti, Ca & O	" "	27 x 50 μ
	3	Si, Ca, Mg, S & O	" "	30 x 50 μ
	4	Si, Zr, Ca, O	" "	25 x 35 μ
	5	Si, Ca, Al, K, Na, Fe, & O	" "	50 μ diameter
	6	Si, Fe, K, Mg, & O	" "	21 x 21 μ
205 A	1	Si, K, Na, Al, Mg, Ca, Fe, & O	alpha-Quartz & sodium calcium aluminum silicate hydrate	300 μ diameter
	2	Si, K, Al, Fe, & O	alpha-Quartz	75 μ diameter
	3	Si, Al, Ca, K, & O	" "	60 x 125 μ
	4	Si, Al, Mg, & O	alpha-Quartz & magnesium aluminum silicate hydrate	100 μ diameter
233*	1	U, O, C, & Nb	UC_2 + uranium oxides	65 micron sphere
	2	Th, O, Si, Al, & K		5 μ
236*	1	U, O, & C	UC_2 + uranium oxides	6 μ
	2	U & C	UC_2	less than 2 μ
	3	U & O	uranium oxide	5 x 15 μ
	4	U & C	UC_2	6 x 12 μ
	5	U & O	uranium oxide	1-2 μ
228 B*	1	Si, K, Ca, Fe, Mg Ti, O, & U		180 μ

*Electron microprobe analysis.

attempted. One sample was washed, dried, and placed in a solution of 1, 1, 2, 2, tetrabromethane (density 2.96). After agitating and centrifuging the sample, two portions, one that settled to the bottom and one that floated on the surface, were radioautographed to determine which had the activity. The activity was found to be in the portion that floated. The settled material was made of iron compounds, as determined on the electron microprobe. This supports the above ideas and data.

No attempt was made to determine correlations or enrichment factors with the gamma data. It was felt that the method of calculation, with the associated error, did not warrant additional calculations to expand the data. Although the data presented are valid, it should be noted there can be a relatively large error associated with each value. Since the least squares method of calculation cannot be applied to isotopes with energies less than 0.1 MeV, ^{147}Nd and ^{239}Np activities could not be calculated. These isotopes were detected by inspection of the spectra.

The electron microprobe data supports the size and density data. Although several particles were reported to have an alpha quartz matrix, reactor material, as verified by radioautograph, was present.

V. INTERPRETATION OF FIELD AND LABORATORY RESULTS

Correlation of activity per unit area and distance demonstrates an exponential decrease of activity with distance, Figure 9. Curve A is the ratio of the total activity (fissions) to the total positive plot area versus distance. Curve B is the ratio of total activity (fissions) to the total plot area surveyed between the extreme edges of the deposition pattern plotted against distance.

It is assumed that larger particles will be deposited closer to the source if all particles are the same density and are ejected to the same height. The average number of fissions per particle is shown in Figure 10 to follow an exponential decrease with distance. If the particle size does vary inversely with distance, as assumed, then this activity per particle to distance relationship indicates a direct correlation of size and activity. Due to the nature of the isolated particles, i.e., shattered pieces, the actual sizes of the particles as they were deposited were not obtained. Because of this, no correlation can be made between measured particle sizes and activity.

A graph of activity (fissions) per unit area versus azimuth from Test Cell C, Figure 11, indicates patterns similar to deposition concentration, Figure 2. The 15-mile arc has a bi-modal pattern, which is similar to the other arcs. The similarity in pattern of the particle concentration curves in Figure 2 and activity concentration in Figure 10 shows that the activity per particle along a given arc was relatively uniform. As expected, there are some

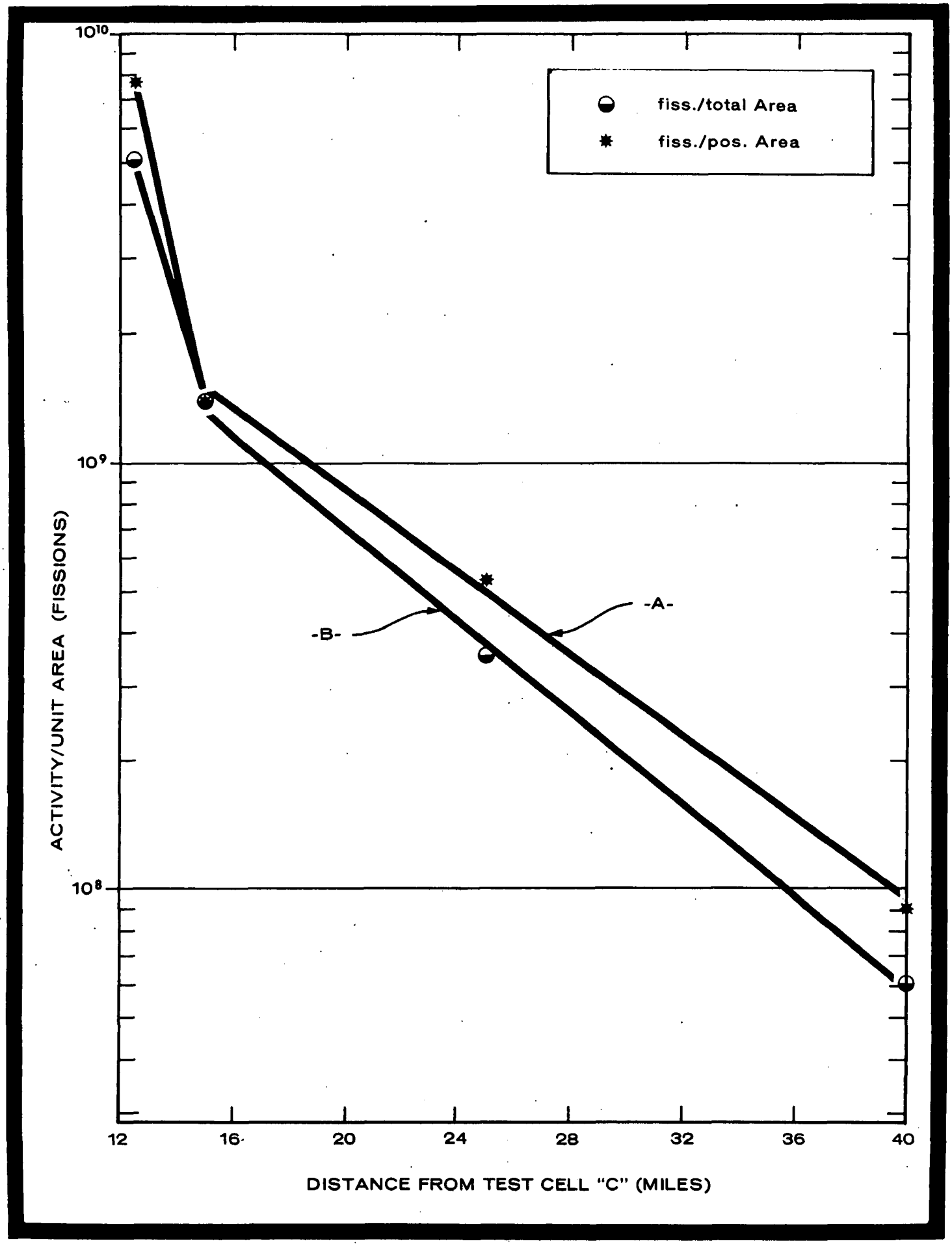

Figure 9. Activity per unit area versus distance.

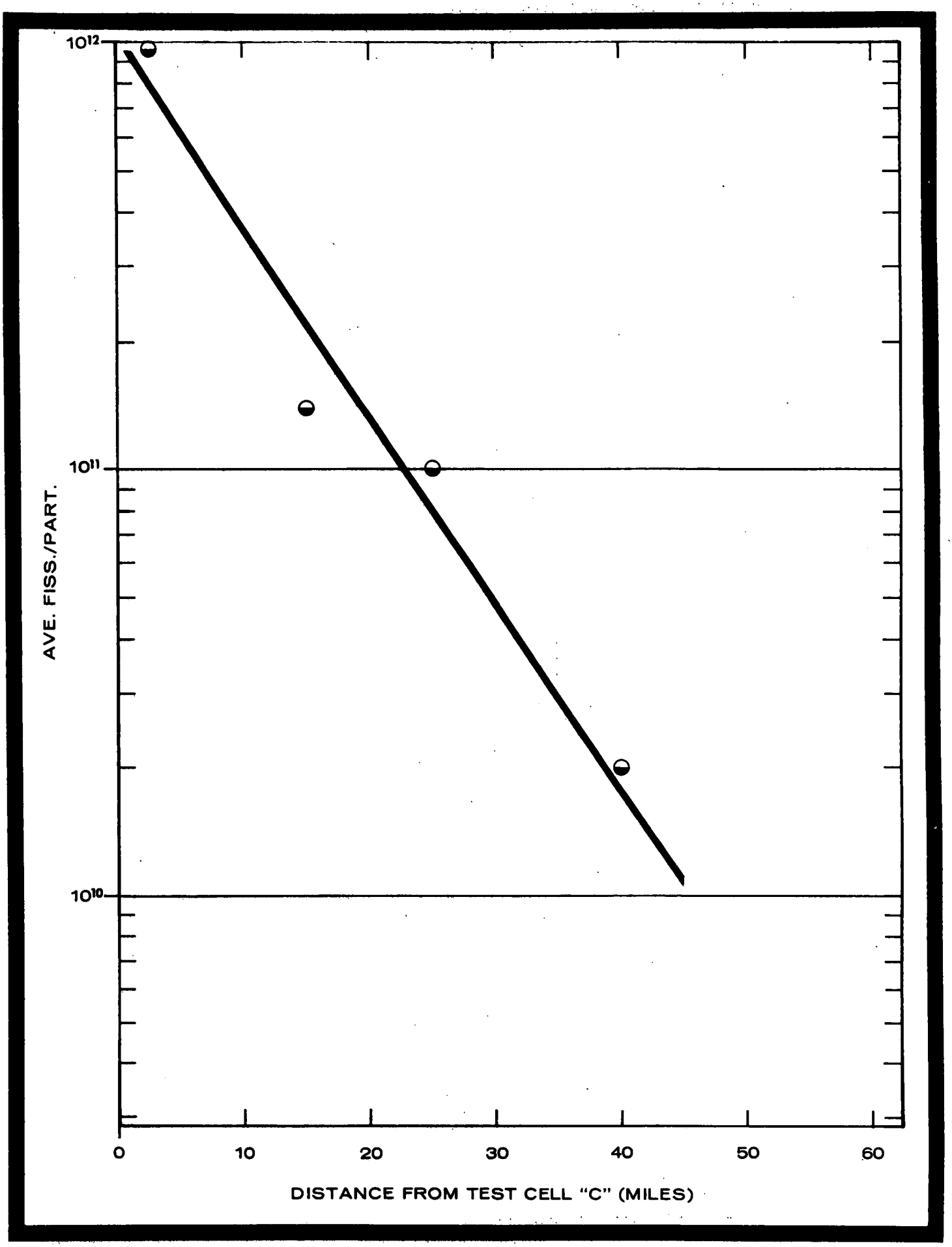

Figure 10. Average activity per particle versus distance.

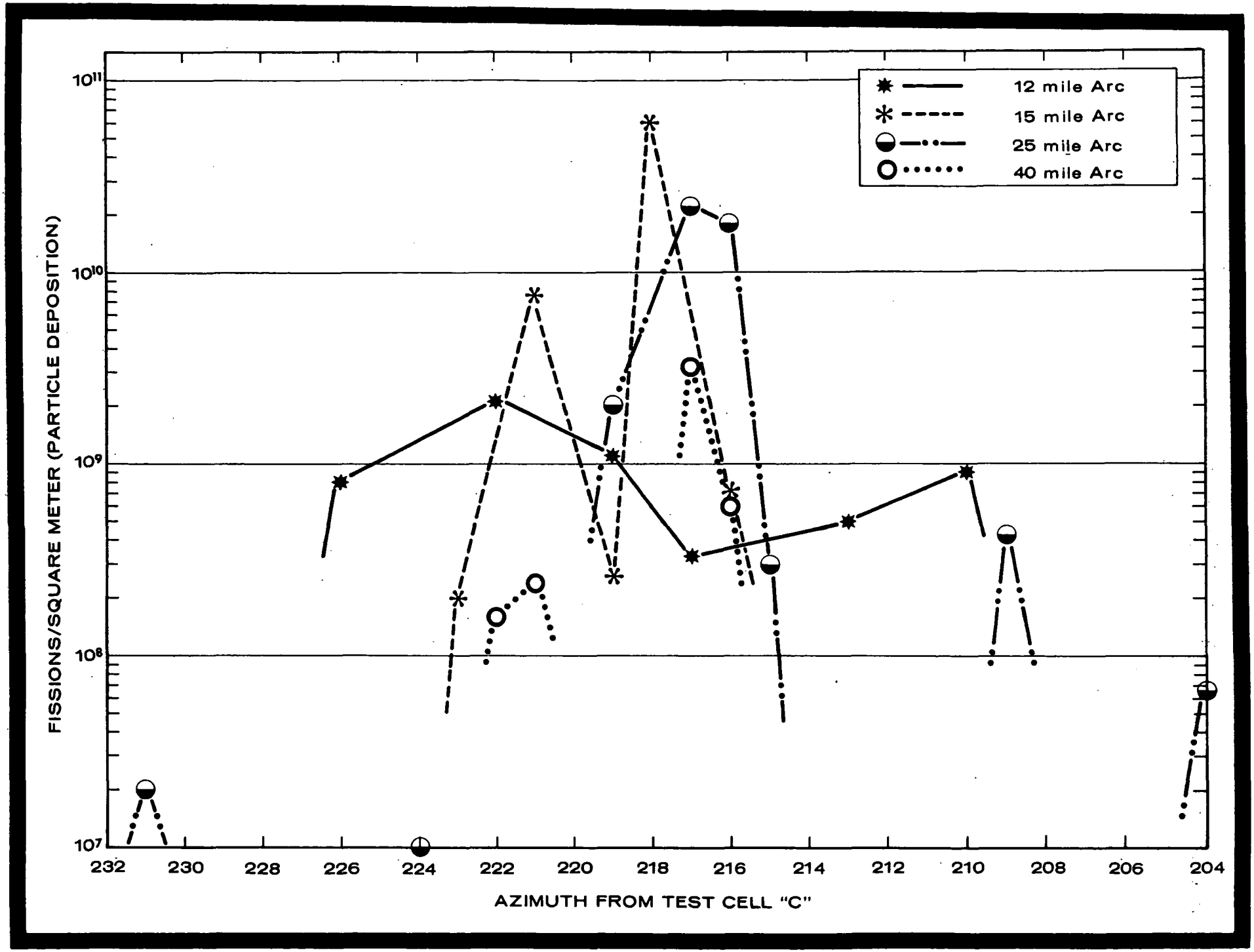

Figure 11. Activity across surveyed arcs.

deviations, notably the low activity per unit area at 219° at 15 miles. Six particles were found at this location, but weather conditions prevented collection of more than three. The three collected were all of low activity. This may also account for the values at 15 miles being low on the curves of Figures 9 and 10.

VI. SUMMARY

Particulate material was located after the NRX-A6 reactor test on a hotline that generally agreed with the second standard level winds. Analysis of the particles indicated they were fragile, had high specific activities, were less dense than reactor core material and were composed of core material and sand. The small number of particles limited definite correlations of particle parameters, but a good indication of the deposition pattern was found.

DEFINITION OF TERMS

Particle - Reactor material, may be beads, shells, flakes, etc., identified as a single hot spot in the survey of a one square meter plot.

Particle Concentration - Number of particles per area, as determined from the survey.

Sample - The volume of material (sand and reactor material) collected with one identifiable hot spot obtained in the field, i.e., Sample 204.

Specimen - The volume of material containing activity from a sample, i.e., 204-A, 204-B, etc., mounted on a 1-by 3-inch glass slide - more than one radioactive specimen may result from a single sample (particle) due to fracturing, separation, etc.

Plot - Each one square meter area that was surveyed at a location.

Location - Place identified by azimuth and distance at which a specific number of one square meter plots were surveyed.

REFERENCES

1. Project Proposal for Reactor Effluent Studies - Particulate August 1, 1967, Environmental Surveillance, SWRHL.

2. Preliminary Report of Off-Site Environmental Surveillance for NRX-A6 Full Power Test, January 1968, SWRHL.

3. Preliminary Report of Aerial Surveillance and Monitoring NRX-A6, EP-III, January 1968, Environmental Surveillance, SWRHL.

4. Synopsis of the Meteorological Conditions Associated with NRX-A6, EP-III, January 1968, U. S. Department of Commerce, Environmental Science Services Administration, Air Resources Laboratory, Las Vegas, Nevada.

5. Calculated Activities and Abundances of ^{235}U Fission Products, R and D USNRDL-456, NSO81-001, by R. C. Bolles and N. E. Ballou.

6. Critical Analysis of Measurement of Gross Fission Product Activity in the Air at Ground Level, NRL 5440, February 1960, Lockhart and Patterson.

APPENDICES

APPENDIX A

SAMPLING INSTRUCTIONS

1. Drive to the designated area.

2. At a distance of at least 50 feet from the road, place a one-meter square template on the ground as many times as necessary to obtain the specified plot area. (Example - on arc at 16 miles, 30 placements of the template would be required).

3. With an E-500B survey instrument, search the area inside each template for hot spots. Trace a path back and forth across the area, sweeping a one-foot-wide path, with the probe held horizontally six inches above the ground. The beta shield is to be open and oriented downward.

4. After a hot spot is found insert a small stake in close proximity to the spot.

5. After surveying the one-meter area, the activity is picked up using laboratory scoops to obtain the smallest amount of material. The activity is placed in small labeled bottles. Fill out a log sheet at each plot indicating the number of particles collected.

6. Move to the next sampling plot and repeat the above procedure.

APPENDIX B

PARTICLE ISOLATION METHOD

The sample contained in a small plastic bottle was emptied into a large planchet. Small portions of the sample were scooped out and checked with the lab monitor. When the small portion contained activity it was subdivided to a minimum amount of material. This material was spread on a 1-by 3-inch glass slide and a 30% collodion solution was used to fix the material to the slide.

After the collodion was dry, the slide was radioautographed (AR'ed) by placing a 1-by 2-inch flap of unexposed X-ray film next to the collodion, holding it in place with a piece of masking tape, Figure B. The slide with the attached film was placed in a light tight exposure holder.

After the exposure period, the slide and the film flap were placed in a rack and developed in small trays with only the film coming in contact with the developing solutions. After drying, the film was folded away from the slide and a small pin hole punched in the center of the dark spot. The dark spot on the filter indicates the location of the radioactive particle in the collodion film. The slide was placed on a microscope stage and the microscope was focused in the center of the pin hole. The stage was lowered and the flap folded back. The stage was raised until the particle came into view. In the event more than one particle (radioactive or non-radioactive) was present in the field of view and the observer was unable to determine the exact radioactive particle, a small area was picked from the slide and transferred to a second slide. A drop or two of collodion was put on the slide and the particles were dispersed

with a pick. The initial slide had a drop of collodion placed where the piece was removed. Both slides were then AR'ed and the above process repeated. After positive identification was made, the particle was located for future reference by starring the collodion around the particle.

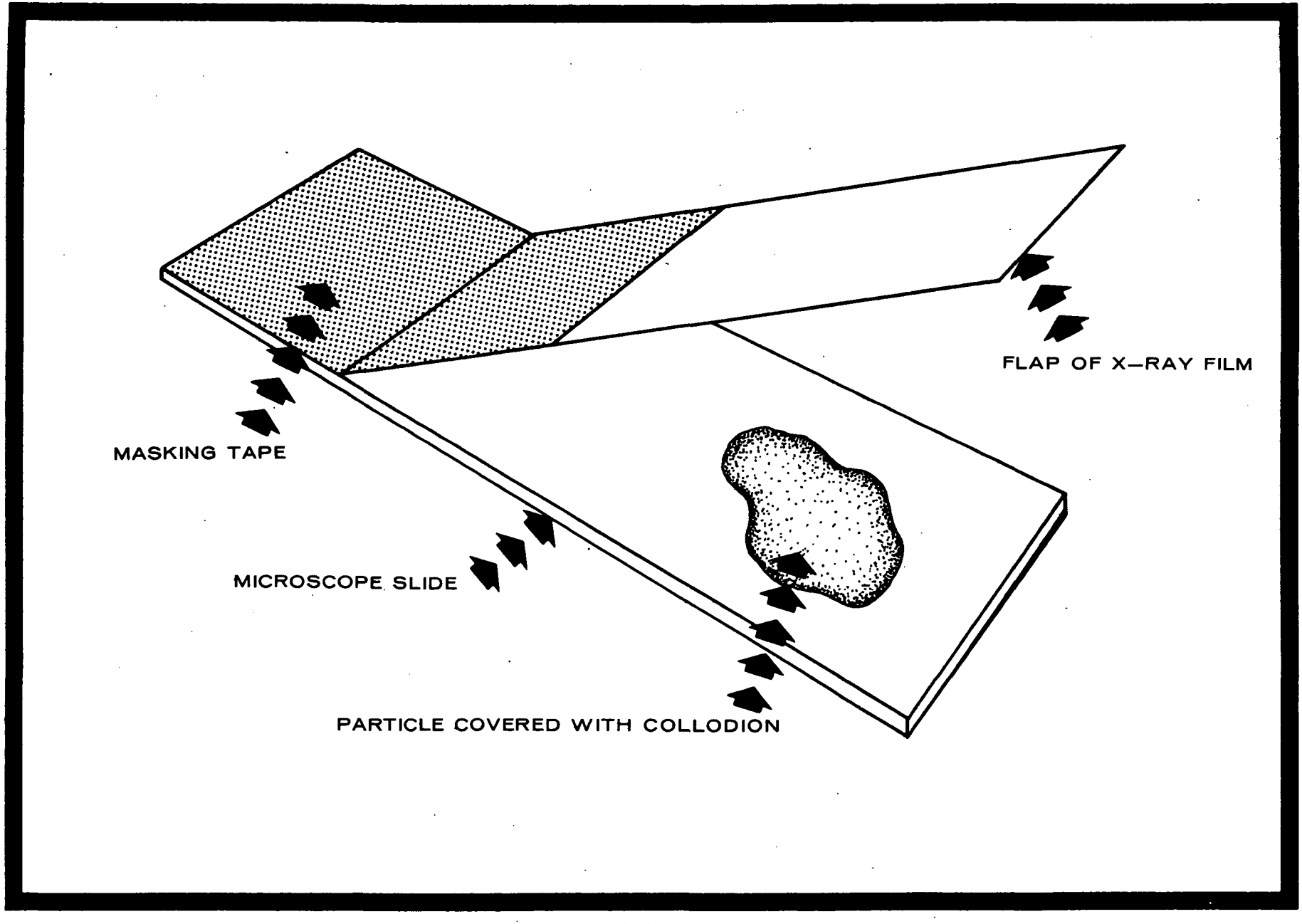

Figure B. Sketch of X-ray film attached to glass slide.

APPENDIX C

BETA COUNTING INFORMATION

Procedure

Samples were counted at various fixed distances from the detectors in order to reduce count rates to minimize resolving time losses. The samples were counted and logged by date and time of count. Counting times of one minute were adequate for all samples. Count rates were corrected for resolving time losses and the data were plotted for decay and absorption.

Equipment

Detector	End window GM
	Atomic Accessories Inc. Model FC-214
	Window - 1.14 mg/cm^2
Scaler	RIDL Model 49-25
Absorbers	Atomic Accessories, Inc. Model AB-23
Sample Holders -	Glass Slide Mounts (microscope)
Standards	^{137}Cs deposited as a point source on glass slide
Resolving Time -	46μ Sec.

APPENDIX C

Table 1. Activities and size of individual specimens.

Sample No.	DPM[1]	Fission[2] (E09)	Pico[3] curies (E03)	Size (μ)
200	94,000	8.7	42	53x50 shell
201	110,000	10	50	120x120
202-A	1,500	0.1	0.7	f/s[4]
202-B	48,000	4.6	21	200x230
203-A	180,000	17	81	200x250
203-B	40,000	3.7	18	Shattered bead
204-A	2,700,000	260	1,200	48x68 (shattered bead)
204-B	4,500	0.4	2	105x93, 50x41, f/s
204-C	19,000	1.7	8.4	50, f/s
204-D	21,000	1.9	9.3	8.8, f/s
204-E	12,000,000	1,100	5,500	105x130
204-F	44,000	4.1	20	15x18, 8.8
204-G	54,000	5	24	42x25, 35x22, 50x50, 12.5
204-H	9,900,000	960	4,500	70x93 (shattered bead)
204-J	8,600,000	850	3,900	100x83 (shattered bead)
204-K	290,000	27	130	f/s
205-A	3,800	0.4	1.7	f/s
205-B	13,000	1.2	5.8	f/s
205-C	1,300	0.1	0.6	f/s
205-D	3,500	0.3	1.6	104x150
205-E	120,000	11	54	4.2, f/s
205-F	110,000	10	50	2.2
205-G	620,000	56	280	100, 150, 140, f/s
205-H	28,000,000	2,700	12,000	100x117, f/s
205-J	4,300	0.4	1.9	f/s
205-K	4,500	0.4	2	280x100

Appendix C (continued)

Table 1. Activities and size of individual specimens (continued).

Sample No.	DPM[1]	Fission[2] (E09)	Pico[3] curies (E03)	Size (μ)
205-L	11,000	1.0	5.1	36x100, 25
205-M	8,400	0.8	3.8	f/s
205-N	71,000	6.6	32	f/s
205-O	8,100	0.8	3.7	Shattered pieces 17-25 μ, 35
205-P	1,500	0.1	0.7	430
205-Q	11,000	1.0	5.1	25, f/s
205-R	7,500	0.7	3.4	8.8, f/s
205-S	8,600	0.8	3.9	6.6, f/s
205-T	17,000	1.6	7.6	f/s
205-U	5,300	0.5	2.4	f/s
205-V	28,000	2.6	13	f/s
205-W	5,000	0.5	2.2	f/s, 140
205-X	31,000	2.9	14	35, 12.5, f/s
205-Y	6,700	0.6	3	44, f/s
206-A	3,800,000	370	1,700	17.5x17.5, 140x150, 70x66, 35x42, 25x25
206-B	440,000	41	200	25, f/s
206-C	860,000	79	390	f/s
207	6,000,000	550	2,700	114 (bead)
208	1,600	0.2	0.7	f/s
209-A	73,000	6.8	33	f/s
209-B	700	0.1	0.3	f/s
209-C	200	0.02	0.1	f/s
209-D	4,900,000	460	2,200	70 (in paper)
210-A	2,300	0.2	1.0	f/s
210-B	2,300	0.2	1.0	f/s

Appendix C (continued)

Table 1. Activities and size of individual specimens (continued).

Sample No.	DPM[1]	Fission[2] (E09)	Pico[3] curies (E03)	Size (μ)
210-C	1,300	0.1	0.6	f/s
210-D	1,100	0.1	0.5	f/s
210-E	160,000	15	70	Shattered piece
211-A	31,000,000	2,900	14,000	Bead (lost)
211-B	2,200	2.0	9.9	165x170, 8.8, (several flakes 9-17μ)
212-B	200	15	0.1	511
212-C	37,000,000	3,500	17,000	239x150
212-D	56,000	5.1	24	On paper[5]
212-E	71,000	6.6	32	On paper[5]
212-F	11,000	1.1	5.1	On paper[5]
213-A	190,000	19	85	f/s
213-B	19,000	1.8	8.6	f/s
213-C	5,200	0.5	2.4	f/s
213-D	15,000,000	1,400	6,900	140 (bead)
214-A	51,000	4.8	23	f/s
214-B	39,000	3.6	17	12.5, f/s
214-C	11,000	1	4.7	f/s
214-D	23,000	2.1	10	4-12μ, f/s
214-E	22,000	2	9.8	25x25
215	230,000	22	100	8.8, f/s
216	1,100	0.1	0.5	185x328
217	6,000	0.6	2.7	f/s
218-A	4,700	0.4	2.1	f/s
218-B	5,400	0.5	2.4	73
218-C	9,300	0.9	4.2	6, 8.5

Appendix C (continued)

Table 1. Activities and size of individual specimens (continued).

Sample No.	DPM[1]	Fission[2] (E09)	Pico[3] curies (E03)	Size (μ)
218-D	1,200	0.1	0.5	390
218-E	1,800	0.2	0.8	1, 1, 3
218-F	23,000	2.2	11	f/s
218-G	2,100	0.2	0.9	f/s
218-H	900	0.1	0.4	f/s
218-J	1,700	0.2	0.8	245
218-K	6,500	0.6	2.9	1.5, 48, 140, 172
218-L	2,100	0.2	0.9	f/s
218-M	1,000	0.1	0.5	Several flakes less than 10 μ
218-N	800	0.1	0.4	561
218-O	2,000	0.2	0.9	220
219-A	18,000,000	1,800	8,100	117 (bead), f/s
219-B	310,000	29	140	42x30
220-A	110,000	11	51	12-17 μ, f/s, 8.5, 12, 230, 130x100, 135, 273
220-B	34,000	3.1	15	185
220-C	800	0.1	0.3	f/s
220-D	6,400	0.6	2.9	48
220-E	58,000	5.4	26	17.5x25
221-A	7,100	0.7	3.2	f/s
221-B	110,000	10	48	f/s
222-A	45,000	4.1	20	f/s
222-B	86,000	8.3	39	f/s
223-A	95,000	8.8	43	160x120 (bead)
223-B	19,000	1.8	8.7	f/s
223-C	1,500	0.1	0.7	f/s

Appendix C (continued)

Table 1. Activities and size of individual specimens (continued).

Sample No.	DPM[1]	Fission[2] (E09)	Pico[3] curies (E03)	Size (μ)
223-D	4,800	0.4	2.2	8-15μ, f/s
223-E	26,000	2.4	12	9.8x12, 8.5x4.2
223-F	19,000	1.8	8.6	12.5, 17, 25
224-A	23,000	2.2	11	8.4x12, 7.1x5
224-B	330,000	30	150	f/s
224-C	250,000	25	120	140x100
224-D	270,000	26	122	12, f/s
224-E	25,000	2.3	11	60, 140, f/s
224-F	290,000	27	130	50x50
224-G	13,000	1.2	6	f/s
224-H	750,000	70	340	f/s
224-J	30,000	2.8	13	f/s, 12.5x12.5
225	440,000	41	200	100x51, 35x31, f/s
226-A	3,000	0.3	1.4	295
226-B	2,600	0.2	1.2	f/s
227-A	300	0.03	0.2	f/s
227-B	900	0.1	0.4	f/s
228-A	19,000	1.7	8.4	f/s
228-B	200,000	18	8.8	70x35, f/s
228-C	26,000	2.4	12	12.5, f/s
228-D	31,000	2.9	14	17.5x6.2, 35x35
228-E	20,000	1.8	9	16x13
228-F	18,000	1.7	8.1	f/s
228-G	11,000	1	5	f/s
228-H	27,000	2.5	12	48x53, f/s
228-J	18,000	1.7	8.1	f/s

Appendix C (continued)

Table 1. Activities and size of individual specimens. (continued)

Sample No.	DPM[1]	Fission[2] (E09)	Pico[3] curies (E03)	Size (μ)
228-K	83,000	7.7	37	f/s
228-L	9,400	0.9	4.2	12x8.5, 3x6, f/s
228-M	12,000	1.1	5.3	f/s
228-N	16,000	1.5	7.1	f/s
228-O	7,800	0.7	3.5	23x36
228-P	8,400	0.8	3.8	13.2x17.5
228-Q	17,000	1.6	7.6	17.5x17.5, 12.5x17.5, f/s
228-R	4,600	0.4	2.1	8.8, f/s
228-S	4,500	0.4	2	f/s
228-T	15,000	1.4	6.7	3, 24,220, f/s
228-U	5,900	0.5	2.7	f/s
228-V	35,000	3.3	16	88, f/s
228-W	22,000	2	9.9	f/s
228-X	15,000	1.4	6.7	f/s
228-Y	42,000	3.9	19	140, 140, f/s
228-Z	9,100	0.9	4.1	145, f/s
229	3,000	0.3	1.4	50x55
230	22,000	2	9.8	95x93 (Shell)
231	2,100,000	190	950	100 (half bead) 75x110
232	35,000	3.3	16	f/s
233	5,600,000	520	2,500	66x63 (shattered bead)
234-A	3,000,000	270	1,300	68
234-B	1,100,000	99	480	40x50
235	140,000	13	63	70x53
236	91,000	8.5	41	Shattered shell 50 pieces $\leq \approx 17.5\,\mu$

Appendix C (concluded)

Table 1. Activities and size of individual specimens (continued).

Sample No.	DPM[1]	Fission[2] (E09)	Pico[3] curies (E03)	Size (μ)
237	60,000	5.5	27	72x100
238-A	2,100	0.2	0.9	f/s
238-B	2,500	0.2	1.1	320
239-A	28,000	2.6	13	< 10 μ, f/s
239-B	1,700	0.02	0.8	f/s
240	1,700,000	160	760	80x110
241	130,000	12	59	12.5x25, f/s
242-A	1,900	0.2	0.8	f/s
242-B	20,000	1.8	8.9	70x75
243	3,400	0.3	1.5	10x8.4
244	3,200	0.3	1.5	130x92, 4.2, f/s
245	4,600	0.4	2.1	f/s
246-A	15,000	1.4	6.6	8.8, f/s
246-B	5,300	0.5	2.4	84x78
246-C	30,000	2.8	14	60x50, f/s

[1] At time of count 12/27/67

[2] E09 = 10^9

[3] E03 = 10^3

[4] Flake on Sand

[5] Particle in paper due to separation process

APPENDIX C

Table 2. Special collected samples*.

Sample No.	Size in μ	Sample No.	Size in μ
100	94x84	127	23x19
101	47x38	128[A]	94x94
102	113x113	129[B]	131x103
103	122x94	130[B]	40x31
104	94x75	131	31x28
105	38x84	132[C]	47x47
106[D]	338x375	133	26x28
107[D]	564x497	134	35x57
108	75x75	135[E]	94x113
109[D]	141x150	136	42x31
110	113x94	137	31x28
111	38x28	138[D]	375x563
112	75x122	139[E]	62x85
113	130x150	140[D]	656x1126
114	94x113	141	109x123
115	141x130	142[C]	94x94
116	75x75	143	31x39
117	113x141	144	54x83
118[D]	281x263	145[E]	92x49
119[D]	319x188	146[B]	77x77
120	94x94	147	31x39
121	122x150	148[B]	37x53
122	113x66	149	15x15
123	94x94	150[E]	94x38
124	12x12	151	19x17
125	15x17	152	22x14

Appendix C (concluded)

Table 2. Special collected samples* (continued).

Sample No.	Size in μ	Sample No.	Size in μ
126	84x75	153	31x31

*3-3.5 miles west of Lathrop Wells on Highway 95.

A - May have sphere attached
B - Smooth surface
C - Spherical
D - Sand grain
E - Sand grain with particle - particle size given

Note: All particles very dark, all particles irregular in shape unless otherwise noted, sizes given are greatest linear dimensions and length perpendicular to greatest linear dimension.

APPENDIX C

Table 3. Isotopic activities for individual specimens[1].

Sample No.	^{91}Sr	^{95}Zr	^{97}Zr	^{99}Mo	^{103}Ru	^{131}I	^{132}Te-I	^{133}I	^{135}I	^{140}Ba-La	^{141}Ce	^{143}Ce
200		1.4 E02		1.5 E04		1.0 E03				4.5 E03		2.7 E05
200**[1]		9.3 E04			8.5 E03					1.7 E02		
202A						1.3 E02				3.4 E02		
202B		5.2 E03		1.6 E05	4.1 E03	2.1 E03	8.4 E03			4.3 E03	5.0 E03	
203A				2.4 E04		1.1 E03				1.4 E04	3.3 E03	
203B		2.6 E02		1.7 E03		3.6 E02				4.6 E03	5.2 E02	
204A-G**[1]		2.2 E05			1.3 E05					3.0 E05	2.1 E05	
204H-K**[1]		1.6 E05			1.2 E05					2.3 E05	1.8 E05	
205A-Y**[1]		2.3 E05			2.0 E05					1.9 E05	3.4 E05	
206A-C**		6.5 E04		3.0 E05	3.4 E04					1.5 E05	5.4 E04	
207		8.0 E04		4.2 E05	3.5 E04	1.8 E04				8.5 E04	1.3 E05	
208				6.0 E02		1.7 E03				1.9 E02		
209A-C**					8.3 E02	2.8 E03				1.3 E04		
209D		8.1 E04			7.2 E04					1.1 E05	8.5 E04	
210A-D**		1.1 E02		4.2 E03		6.5 E03				5.8 E02	8.5 E01	
210E		1.3 E03				1.5 E03				3.0 E04		
211A		6.1 E05		1.0 E07	2.6 E05	3.1 E05	1.3 E06			6.0 E05	6.9 E05	
211B**[1]		2.0 E05			1.1 E05					5.6 E03	9.3 E04	
212B				5.7 E03		9.3 E02				3.8 E02		
212C-F**		2.2 E05		3.6 E06	1.1 E05	7.8 E04				2.0 E05	3.0 E05	
213A-C				1.7 E05	2.5 E03	5.8 E03				3.7 E04		
213D		2.5 E05		1.3 E06	1.0 E05	8.3 E04				2.3 E05	3.0 E05	
214A-E					1.4 E03	2.5 E03	5.6 E03			2.5 E04		
215						4.0 E03				5.7 E04		

Appendix C (continued)

Table 3. Isotopic activities for individual specimens[1]. (continued)

Sample No.	^{91}Sr	^{95}Zr	^{97}Zr	^{99}Mo	^{103}Ru	^{131}I	^{132}Te-I	^{133}I	^{135}I	^{140}Ba-La	^{141}Ce	^{143}Ce
216		5.0 E02	6.3 E04	1.4 E03	1.1 E02	1.0 E02				1.8 E02	2.6 E02	9.3 E03
217				7.9 E03		3.0 E02				1.6 E03	2.5 E02	
218A	3.7 E04			1.0 E04		1.1 E03	1.2 E03	4.8 E03		4.8 E02	1.0 E02	
218B	4.9 E04			9.3 E03		4.8 E03	2.9 E03	3.6 E04		3.7 E02	2.4 E02	
218C	6.1 E04	3.6 E02	2.0 E04	6.5 E02		1.1 E02			4.1 E04	4.9 E02	4.8 E02	1.8 E04
218D	1.3 E04	1.1 E02	2.2 E04	3.6 E02		1.4 E02			3.1 E04	1.1 E02	8.2 E01	2.5 E03
218E	6.0 E04	6.5 E01	4.2 E03	4.3 E02		1.4 E02	1.2 E03	1.4 E03	7.8 E03	6.8 E01	6.5 E01	2.2 E03
218F	2.5 E05	2.6 E02	2.2 E04	5.8 E04		3.8 E03	1.3 E04	2.6 E04		2.2 E03	2.1 E03	2.6 E03
218G	1.6 E04	1.4 E02	6.4 E03	1.9 E04		1.4 E03	2.6 E03	6.4 E03	2.0 E04	7.1 E04	4.3 E02	3.4 E03
218H	9.3 E03	6.0 E01	3.3 E03	1.4 E02					6.3 E03	4.6 E01	5.0 E01	2.5 E03
218J	6.8 E04							1.1 E03		1.4 E02		
218K	3.2 E03			6.0 E02		2.9 E02	3.8 E03	1.0 E03		1.0 E03	1.7 E02	5.0 E02
218L	6.2 E03			6.0 E02		5.5 E01	5.6 E02	4.4 E02		3.7 E02		
218M	1.1 E04	8.5 E01	5.1 E03	1.0 E02					6.4 E03		7.1 E01	3.6 E03
218N	1.6 E04		1.3 E03	1.7 E03		9.3 E01	1.4 E03			2.9 E02	2.6 E02	
218O	1.5 E03		7.0 E02	1.6 E02		1.0 E02	9.3 E02			3.1 E02	1.0 E02	7.0 E02
219A		2.2 E05			1.1 E05					1.7 E05	2.7 E05	
219B		2.9 E04		9.3 E04	2.8 E03					2.0 E04	2.7 E04	
220A-D**				5.7 E04	1.1 E03	2.3 E03				2.1 E04		
220E						1.5 E03	2.9 E03	1.3 E05		1.6 E04		
221A		7.3 E01		2.0 E03		2.6 E02				1.7 E03		
221B		6.3 E03		4.8 E04	1.3 E03	3.9 E03				2.9 E04	1.1 E03	
222A		1.3 E02		4.8 E02		6.7 E02	2.1 E03	7.3 E04		1.0 E04		
222B		5.7 E02		1.6 E04		1.4 E03				2.3 E04		
223A-D**		2.9 E03		5.4 E04	1.2 E03	2.4 E03				1.8 E04	1.4 E03	
223E						3.0 E02		5.5 E03		6.0 E03		
223F		6.1 E01		5.0 E02		1.8 E02				4.2 E03		

Appendix C (continued).

Table 3. Isotopic activities for individual specimens[1]. (continued)

Sample No.	^{91}Sr	^{95}Zr	^{97}Zr	^{99}Mo	^{103}Ru	^{131}I	^{132}Te-I	^{133}I	^{135}I	^{140}Ba-La	^{141}Ce	^{143}Ce
224A		9.3 E02		3.8 E03						3.2 E03	2.6 E03	
224B-F**		5.8 E03		1.1 E05	8.2 E03	7.3 E03				1.8 E05		
224G				5.2 E03		7.2 E02		1.6 E05		8.5 E03		
224H				2.5 E05	6.1 E03	1.4 E04				3.5 E04	3.0 E03	
224J		3.2 E02		1.2 E05		8.5 E02				4.1 E03	3.2 E03	
225		3.0 E04		5.5 E04						3.8 E04	2.5 E04	
226A	2.2 E04			4.7 E02		2.5 E02	6.2 E03			2.4 E02	7.8 E01	
226B	4.3 E04		3.4 E03	2.1 E03		5.2 E02	2.4 E03	3.4 E03	1.3 E04	3.4 E02	1.0 E02	
227A	1.6 E04			7.3 E03		3.3 E02	1.4 E02	3.1 E03				
227B	1.2 E04		1.4 E03	2.1 E04		9.3 E02	5.0 E02	6.0 E03	4.3 E04	9.3 E01	2.6 E02	
228A		1.3 E03	1.5 E05	2.8 E03		1.1 E02				3.6 E03	4.3 E02	2.5 E04
228B				2.7 E03			2.2 E03			4.2 E04	1.5 E03	
228C		9.3 E02		8.5 E03		1.0 E03				4.6 E03	4.8 E02	
228D		2.5 E02	3.2 E04	1.6 E03		8.3 E02				5.4 E03		1.2 E04
228E						3.7 E02		8.3 E04		3.5 E03		
228F				5.1 E03		1.1 E02		5.9 E04		4.7 E03		
228G						2.6 E02	3.6 E02	1.4 E04		2.0 E03	1.7 E02	
228H		3.8 E02	6.9 E04	6.6 E03		1.4 E02		6.6 E04		5.3 E03		1.2 E04
228J	1.2 E07	3.8 E02		2.8 E03		3.8 E02				3.1 E03	8.4 E02	
228K		8.5 E02		3.6 E03		4.7 E02				3.4 E03	1.7 E03	3.4 E04
228L		1.7 E01	9.3 E04	2.7 E03		9.3 E01				1.2 E03	9.3 E02	2.1 E04
228M		4.2 E02		5.0 E03		5.0 E02	1.1 E03			2.7 E03	5.7 E02	
228N		1.9 E01	6.6 E04	2.5 E03						7.3 E02	1.1 E03	2.8 E04
228O		3.7 E02	3.7 E04	9.5 E02		1.4 E02				7.5 E02	3.1 E02	1.9 E04
228P				9.3 E02		3.1 E02		4.0 E04		2.2 E03	9.3 E01	
228Q		1.2 E01	5.7 E04	2.9 E03						2.5 E03	8.2 E02	
228R		5.0 E02	4.1 E04	5.0 E02		8.4 E01				4.5 E01	5.3 E02	8.5 E03
228S-Z**		3.8 E03		4.3 E04		2.0 E03				1.4 E04	4.9 E03	
229		2.5 E03	3.4 E05	3.5 E04		8.5 E01				9.3 E02	1.2 E03	3.5 E04
230		2.1 E04		7.8 E04		5.0 E03				1.7 E04	1.5 E04	

Appendix C (concluded)

Table 3. Isotopic activities for individual specimens[1], (continued).

Sample No.	^{91}Sr	^{95}Zr	^{97}Zr	^{99}Mo	^{103}Ru	^{131}I	^{132}Te-I	^{133}I	^{135}I	^{140}Ba-La	^{141}Ce	^{143}Ce
231		6.6 E04		6.2 E05	1.3 E04					2.8 E04	5.5 E04	
232		3.5 E03		1.7 E04		3.4 E02				3.2 E03	4.5 E03	
233		7.9 E04		1.3 E06	2.4 E04					7.1 E04	8.5 E04	
234A**[1]		7.1 E04			2.0 E04					1.1 E05	7.3 E04	
234B		1.1 E05		1.2 E05	8.1 E03					8.5 E04	1.1 E05	
235		2.0 E04		1.4 E05						3.0 E03	1.0 E04	9.3 E05
236**[1]		2.0 E05			6.2 E04					1.4 E05	1.2 E05	
237				4.2 E05						7.3 E04	7.6 E04	
238A-B		2.1 E02		4.8 E02		2.6 E02	1.3 E03			1.0 E03		
239A					2.7 E02	2.5 E02				4.1 E03		
239B												
240		1.8 E05		2.1 E07	2.1 E04					1.4 E05	1.5 E05	
241				2.8 E04								6.0 E05
242A		7.7 E02		1.7 E03						6.0 E01	3.2 E02	1.4 E04
242B		6.1 E03		4.1 E03							2.2 E03	
243	5.7 E04	2.2 E03	1.4 E05	1.3 E04	1.5 E03					1.3 E02	3.2 E02	4.2 E04
244		7.4 E02		2.4 E03		1.7 E02	5.2 E02			2.0 E03		
245		1.9 E02			1.4 E02	5.0 E02				4.0 E03		
246A				2.7 E03		2.9 E02	4.2 E02	4.2 E04		4.9 E03		
246B	4.5 E06					2.2 E02	7.0 E02			1.2 E03		
246C		5.0 E02		3.0 E03	3.2 E02	8.5 E02				6.8 E03		

1 = pCi @ 1200 hours 12-15-67
**[1] = Grouped in one sample holder
** = Grouped in one sample holder (hand calculation)
E02 = $x10^2$

APPENDIX D

DENSITY ANALYSIS METHODS

Selected particles were weighed and their fall velocity in a liquid was observed to determine their density.

The particles were weighed on a Cahn Electobalance in the following manner. The particles were loosened from the slide with a small quantity of amyl acetate. The particles were either lifted or pushed from the slide onto a previously weighed balance boat using a small pick. The mass of the pan and dry particle was then recorded. The particle was then pushed or lifted from the balance pan with a pick, placed back on the microscope slide and fixed again with another drop of collodion.

The fall velocity of the particles was determined as follows. The particle on each slide was first loosened with a drop of amyl acetate. Each slide containing the particle in question was then lowered into the solution of ethyl alcohol. The particle was observed to fall from the slide, and the time of fall was measured using two independent stop watches. The fall velocity was calculated using the average of the two times. Recovery of the individual particles for a second fall time, etc., was not feasible.

Standard particles were used to calibrate the solution because it is known that a departure from the Stokes settling velocity occurs with particles greater than 50 μ in size. The particles used were whole reactor beads, spherical in shape. The composition of these beads according to present calculations is a core of uranium carbide (UC_2), density 11.28 gm/cm^3, surrounded by a reported uniform 25 μ thickness of pyrolytic carbon, density 2.0 gm/cm^3. The results of this calibration are presented in the following table.

APPENDIX D

Table 1. Density analysis calibration data.

Radius (μ)	Weight (μg)	Distance of fall (cm)	Time of fall (sec)	Fall velocity (cm/sec)	Viscosity (cp)
65.9	4.00	21.11	27.5	.77	2.49
68.8	6.25	21.11	-	-	2.49
81.4	14.75	21.11	9.5	2.22	2.49
94.9	15.00	21.11	8.5	2.98	2.49
77.5	5.75	21.11	14.5	1.46	2.49

- = Not reported.

DISTRIBUTION

1 - 13	National Environmental Research Center, Las Vegas, Nevada
14	Mahlon E. Gates, Manager, AEC/NVOO, Las Vegas, Nevada
15	Robert H. Thalgott, AEC/NVOO, Las Vegas, Nevada
16	Henry G. Vermillion, AEC/NVOO, Las Vegas, Nevada
17	Donald W. Hendricks, AEC/NVOO, Las Vegas, Nevada
18	Robert R. Loux, AEC/NVOO, Las Vegas, Nevada
19	Mail & Records, AEC/NVOO, Las Vegas, Nevada
20	Technical Library, AEC/NVOO, Las Vegas, Nevada
21	Chief, NOB/DNA, AEC/NVOO, Las Vegas, Nevada
22	Harold F. Mueller, ARL/NOAA, AEC/NVOO, Las Vegas, Nevada
23	Howard G. Booth, ARL/NOAA, AEC/NVOO, Las Vegas, Nevada
24	D. Gabriel, SNSO, Washington, D. C.
25	George P. Dix, SNSO, Washington, D. C.
26 - 29	Richard A. Hartfield, SNSO-N, NRDS, Jackass Flats, Nevada
30	William C. King, LLL, Mercury, Nevada
31	James E. Carothers, LLL, Livermore, California
32	Ernest A. Bryant, LASL, Los Alamos, New Mexico
33	Harry S. Jordan, LASL, Los Alamos, New Mexico
34	Charles I. Browne, LASL, Los Alamos, New Mexico
35	W. S. Wilgus, NRTO, NRDS, Jackass Flats, Nevada
36	Eastern Environmental Radiation Facility, EPA, Montgomery, Ala.
37	Donald R. Martin, Pan Am. World Airways, Jackass Flats, Nevada
38	Martin B. Biles, DOS, USAEC, Washington, D. C.
39	J. Doyle, EG&G, Las Vegas, Nevada
40	Richard S. Davidson, Battelle Memorial Institute, Columbus, Ohio
41	Carter D. Broyles, Sandia Laboratories, Albuquerque, New Mexico
42	Maj.Gen. Frank A. Camm, DMA, USAEC, Washington, D. C.
43	Stanley M. Greenfield, Assistant Administrator for Research & Monitoring, EPA, Washington, D. C.
44	William D. Rowe, Deputy Assistant Administrator for Radiation Programs, EPA, Rockville, Maryland

DISTRIBUTION (continued)

45 Ernest D. Harward, Acting Director, Division of Technology Assessment, Office of Radiation Programs, EPA, Rockville, Maryland

46 - 47 Charles L. Weaver, Dir., Field Operations Div., Office of Radiation Programs, EPA, Rockville, Maryland

48 Gordon Everett, Dir., Office of Technical Analysis, EPA, Washington, D. C.

49 Library, EPA, Washington, D. C.

50 Kurt L. Feldmann, Managing Editor, Radiation Data & Reports, Office of Radiation Programs, EPA, Rockville, Maryland

51 Regional Radiation Representative, EPA, Region IX, San Francisco, California

52 Arden E. Bicker, REECo, Mercury, Nevada

53 John M. Ward, President, Desert Research Institute, University of Nevada, Reno, Nevada

54 - 55 Technical Information Center, USAEC, Oak Ridge, Tennessee (For public availability).